REPORT DOCUMENTATION PAGE

1. REPORT DATE (DD-MM-YYYY) 28-06-2004	2. REPORT TYPE REPRINT	3. DATES COVERED (From - To)

4. TITLE AND SUBTITLE
Unusual ionospheric echoes with high velocity and very low spectral width observed by the SuperDARN radars in the polar cap during high geomagnetic activity

5a. CONTRACT NUMBER

5b. GRANT NUMBER

5c. PROGRAM ELEMENT NUMBER
61102F

6. AUTHOR(S)
Nozomu Nishitani*, Mark Lester**, Steve E. Milan**, Takahiko Ogawa*, Natsuo Sato,+ Hisao Yamagilshi,+ Akira Sessai Yukimatu,+ and Frederick J. Rich

5d. PROJECT NUMBER
2311

5e. TASK NUMBER
`SD

5f. WORK UNIT NUMBER
A3

7. PERFORMING ORGANIZATION NAME(S) AND ADDRESS(ES)
Air Force Research Laboratory/VSBXP
29 Randolph Road
Hanscom AFB, MA 01731-3010

8. PERFORMING ORGANIZATION REPORT NUMBER
AFRL-VS-HA-TR-2004-1140

9. SPONSORING/MONITORING AGENCY NAME(S) AND ADDRESS(ES)

10. SPONSOR/MONITOR'S ACRONYM(S)

11. SPONSOR/MONITOR'S REPORT

12. DISTRIBUTION/AVAILABILITY STATEMENT
Approved for public release; distribution unlimited

20040715 120

14. ABSTRACT
The spectral width of th ionospheric backscatter echoes obtained with the SuperDARN radars has been regarded as a useful tool for locating specific ionospheric regions such as the cusp. In this paper we report the presence of ionospheric echoes with high (>450 m/s) Doppler velocity and very low (<60 m/s) spectral width obsreved by the CUTLASS and Syowa East and South SuperDARN radars. These echoes have the following characteristics. (1) They have a close correlation with geomagnetic activity such that as the Dst index decreases, the radars tend to observe ionospheric echoes with high Doppler velocity and very low spectral width more frequently. (2) Their existence does not depend on magnetic local time. (3) They are located preferably in the polar cap region, where antilsunward convection prevails. (4) They sometimes exist over a wide range, so thay are more likely to be F-region than E-region echoes. The occurrence of these echoes during active periods is accociated with the suppression of the electric field turbulence. The present result appears consistent with the previous paper by Golovchanskya et al. [2002], who showed the negative correlation between the elctric field turbulence level and geomagnetic activity.

15. SUBJECT TERMS
Electric fields Magnetospheric storms and substorms Polar cap ionosphere Magnetic field configuration
SuperDARN Ionospheric dynamics Low spectral width echoes
Polar cap ionosphere Ionosphere/magnetosphere interactions Electric field turbulence

16. SECURITY CLASSIFICATION OF:			17. LIMITATION OF ABSTRACT	18. NUMBER OF PAGES	19a. NAME OF RESPONSIBLE PERSON
a. REPORT UNCL	b. ABSTRACT UNCL	c. THIS PAGE UNCL	UNL		Frederick J. Rich

19b. TELEPHONE NUMBER (Include area code)
(781) 377-3857

Unusual ionospheric echoes with high velocity and very low spectral width observed by the SuperDARN radars in the polar cap during high geomagnetic activity

Nozomu Nishitani,[1] Mark Lester,[2] Steve E. Milan,[2] Tadahiko Ogawa,[1] Natsuo Sato,[3] Hisao Yamagishi,[3] Akira Sessai Yukimatu,[3] and Frederick J. Rich[4]

[1] The spectral width of the ionospheric backscatter echoes obtained with the SuperDARN radars has been regarded as a useful tool for locating specific ionospheric regions such as the cusp. In this paper we report the presence of ionospheric echoes with high (>450 m/s) Doppler velocity and very low (<60 m/s) spectral width, observed by the CUTLASS and Syowa East and South SuperDARN radars. These echoes have the following characteristics. (1) They have a close correlation with geomagnetic activity such that as the Dst index decreases, the radars tend to observe ionospheric echoes with high Doppler velocity and very low spectral width more frequently. (2) Their existence does not depend on magnetic local time. (3) They are located preferably in the polar cap region, where antisunward convection prevails. (4) They sometimes exist over a wide range, so they are more likely to be F-region rather than E-region echoes. The occurrence of these echoes during active periods is associated with the suppression of the electric field turbulence. The present result appears consistent with the previous paper by *Golovchanskaya et al.* [2002], who showed the negative correlation between the electric field turbulence level and geomagnetic activity. *INDEX TERMS:* 2411 Ionosphere: Electric fields (2712); 2431 Ionosphere: Ionosphere/magnetosphere interactions (2736); 2475 Ionosphere: Polar cap ionosphere; 2788 Magnetospheric Physics: Storms and substorms; 2437 Ionosphere: Ionospheric dynamics; *KEYWORDS:* SuperDARN, polar cap ionosphere, low spectral width echoes, magnetospheric magnetic field configuration, electric field turbulence, geomagnetic storm

1. Introduction

[2] SuperDARN HF radars have been regarded as useful tools for monitoring plasma convection over a large spatial extent with high time resolution [*Greenwald et al.*, 1995]. The main aim of the SuperDARN was to monitor the large-scale electric field in the polar ionosphere over a global extent.

[3] On the other hand, the spectral width of the Doppler spectrum obtained with the SuperDARN radars has been regarded as a powerful tool for monitoring the perturbation level of the ionospheric convection velocity. For example, *Baker et al.* [1995] studied the characteristics of the spectral width of the ionospheric echoes in the noon sector. They

found that the spectral width becomes larger in the cusp region (and possibly in the low-latitude boundary layer). They ascribed the increase in the spectral width to the presence of the electric field turbulence. *Hosokawa et al.* [2002] made a statistical study of the interhemispheric comparison of the spectral width in the dayside sector, and found that the profiles of spectral widths near the cusp region have similar characteristics in both hemispheres.

[4] The spectral width distributions have also been studied in the nightside region. *Lewis et al.* [1997] studied the characteristic of spectral width in the nightside region and reported that the spectral width is high in the higher-latitude nightside auroral oval. *Woodfield et al.* [2002] studied the statistical distribution of the spectral width observed by the Co-operative U.K. Twin Located Auroral Sounding System (CUTLASS) and Syowa SuperDARN radars and found that the spectral width profile has peaks on both open and closed field lines, more complicated than the previous result by *Lewis et al.* [1997]. *Fukumoto et al.* [1999] found weak positive correlation between the Doppler velocity and the Doppler spectral width, suggesting that the electric field is another factor for determining the Doppler spectral width.

[5] Although the spatial distribution of the spectral width characteristics has been extensively studied, there have been

[1]Solar-Terrestrial Environment Laboratory, Nagoya University, Toyokawa, Japan.
[2]Department of Physics and Astronomy, University of Leicester, Leicester, UK.
[3]National Institute of Polar Research, Tokyo, Japan.
[4]Air Force Research Laboratory, Space Vehicles Directorate, Hanscom Air Force Base, Massachusetts, USA.

few studies of the temporal variation of the spectral width, especially the dependence on geomagnetic activity. In this paper we show statistical results of the relationship between the spectral width and geomagnetic activity. In particular, we show the presence of ionospheric echoes with very low spectral width during high geomagnetic activity and then discuss their generation mechanisms.

2. Instrumentation

[6] The data used in this study were obtained by the CUTLASS and Syowa East and Syowa South HF radars from 1 January 1998 to 31 December 2001. The fields of view of the radars are shown in Figure 1. The magnetic latitude and longitude are given in the Altitude Adjusted Corrected Geomagnetic Coordinate (AACGM) system, which is an updated version of the PACE geomagnetic coordinate system [Baker and Wing, 1989]. Magnetic local time (MLT) of the Syowa Station and Iceland is approximately the same as the universal time (UT), and that of the Finland radar is about 3 hours ahead of UT. Beam 7 of Syowa East and beam 3 of Iceland East are approximately conjugate to each other.

[7] In the event study, the ion driftmeter data from the DMSP-F13 satellite at an altitude of approximately 848 km are used to examine the electric field turbulence level. In addition, Polar MFE data are used to examine the magnetic field configuration in the nightside magnetosphere during the period of event study. We also use the geomagnetic field data from International Monitor for Auroral Geomagnetic Effects (IMAGE) magnetometer chain, 210° Magnetic Meridian (MM) chain [Yumoto et al., 2001], and Geophysical Institute Magnetometer Array (GIMA) in the Alaskan region to examine geomagnetic activity for the event study analysis.

3. Analysis Results

[8] In this section we show the result of the data analysis. This section consists of three parts. First, we describe the result of statistical analysis of the spectral width as a function of geomagnetic activity. Then we will study one event where we observed echoes with very low spectral width. Finally, we will show the statistical analysis of the conditions under which ionospheric echoes with very low spectral width are observed.

3.1. Statistical Result: Dependence of the Spectral Width on the Geomagnetic Activity

[9] In this subsection we use the Syowa East beam 7 data, centered in the radar field of view. We will also use the Iceland East beam 3 data, which is approximately conjugate to the Syowa East beam 7.
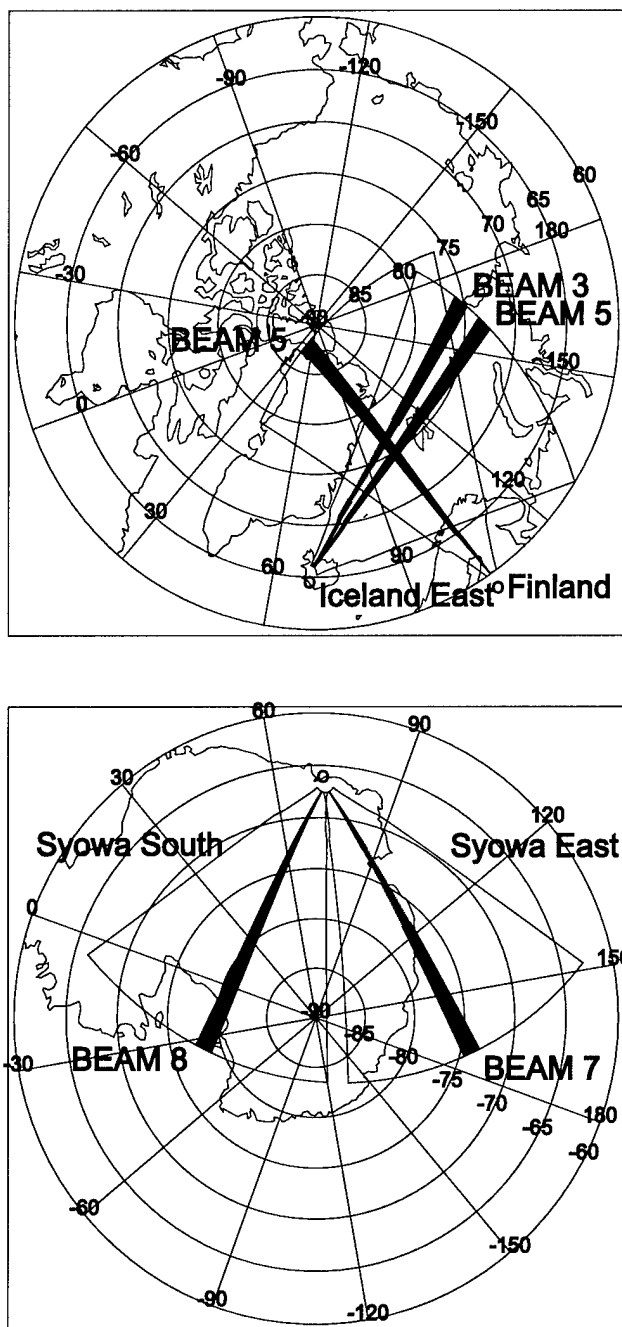
[10] In order to exclude the ground scatter echoes and the interference, we used the noise reduction technique [Fukumoto et al., 1999]. The following types of echoes were identified and used in the present study: (1) echoes detected at more than 3 consecutive radar range gates (~90 km) and lasting for more than 2 min (usually for at least two radar scans), and at the same time (2) echoes with Doppler velocities that increase or decrease monotonically over three consecutive range gates or that exhibit a small difference

(≤33%) between adjacent range gates. In addition, data satisfying at least one of the following criteria was excluded from the study: (1) an echo power of below 0 dB or above 30 dB, (2) a Doppler velocity beyond ±1000 m/s, or (3) a spectral width of above 1000 m/s. We also excluded echoes with the absolute values of Doppler velocities less than 100 m/s and the Doppler spectral width less than 100 m/s in order to remove the effect of possible ground scatter echoes. Only data satisfying none of the above criteria was used in our analysis.

[11] Although the range dependence of the Doppler spectral width is relatively small [Hosokawa et al., 2002; Woodfield et al., 2002; Villain et al., 2002], we limited the range of the data used in the present statistical study to 1000–2000 km. This is in order to reduces the chances that E-region scatter echoes will contaminate the data as such echoes, which tend to be observed in the closer (<500 km) ranges [Hanuise et al., 1991], and also at farther ranges (>2000 km) [Milan et al., 1997; Chisham and Pinnock, 2001] due to the multihop path of the radar wave. For this range, the absolute values of the magnetic latitude of the echo region in both hemispheres are 72 to 77 degrees. Details of the effect of E-region echoes at farther ranges will be discussed in section 4. The MLT of the echo region is about 1–2 hours ahead of the radar site and approximately 1–2 hours ahead of UT.

[12] Figure 2 shows the overall relationship of the Doppler plasma velocity and the spectral width of the ionospheric backscatter echoes obtained by the Syowa East radar for the period of 1 January 1998 to 31 December 2001. The darkness of each bin indicates the detection probability of ionospheric echoes for the specific velocity (every 50 m/s) and spectral width (every 20 m/s) range. The blank area at the bottom center of the plot is the result of excluding possible ground scatter echoes. The solid line indicates the peak values of Doppler spectral widths for each velocity range (except for −100 to 100 m/s). There is a weak positive correlation between the absolute value of the Doppler velocity and the spectral width, consistent with Fukumoto et al. [1999]. This result is natural considering that the turbulence level of the convection velocity normally increases monotonously with the background convection speed.

[13] On the other hand, this pattern changes with geomagnetic activity. Figure 3 shows the relationship between Doppler velocity and the spectral width during high geomagnetic activity (Dst < −90 nT). Obviously, the peak value of the spectral width is shifted towards lower values, especially for higher Doppler velocity ranges. This is more clearly demonstrated in Figure 4a, showing the distribution of the spectral width of ionospheric backscatter echoes for |vel| >= 450 m/s, binned for Dst ranges every 15 nT. We selected the ionospheric echoes with the Doppler speed larger than 450 m/s in order to reduce the effects of ground scatter echoes, centered around 0 m/s, and possibly type 1 E-region echoes, distributed mainly within ±400 m/s [Hanuise et al., 1991]. With the increase of Dst, the peak of the spectral width distribution shifts from higher to lower Doppler spectral widths. For the Dst range less than −90 nT, most of the distributions of the Doppler spectral widths were concentrated between 0 and 100 m/s.

[14] Next we examined the characteristics of the spectral width depending on the relative location of the echo region to the convection pattern. Since beam 7 of the Syowa East radar is aligned nearly in the geomagnetic east-west direction, it is easy to determine whether the region of interest is located in the polar cap (antisunward flow region) or in the auroral zone (sunward flow region), in the dusk and dawn sectors, if we assume two-cell convection pattern (this is highly plausible during high geomagnetic activity).
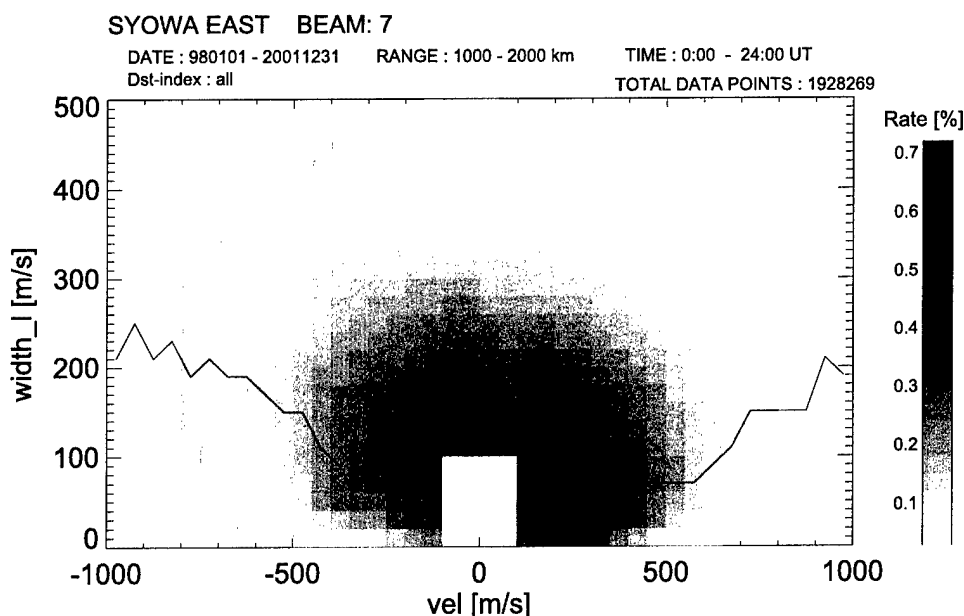
[15] In the antisunward flow region where the echo region is expected to be in the polar cap (Figure 4b) the tendency is obvious, except for one Dst range cell (−135 to −150 nT). On the other hand, in the sunward flow region where the echo is expected to be in the auroral zone (Figure 4c) the effect of geomagnetic activity is rather weak. Therefore it is likely that the echoes with low spectral width are observed preferably in the polar cap region. We obtained the same result by using beam 3 of the Iceland East radar data (Figures 5a and 5b). The overall shift of the distribution of the spectral width toward lower values during higher geomagnetic activity is easily recognizable in Figure 5a (polar cap) whereas this tendency is not so clear in Figure 5b (auroral zone). Figure 5c shows the distribution of the spectral width as a function of Dst index, for the radar range of 2000 to 3400 km. The tendency is the same as Figure 5a, although the number of data points is relatively small.

3.2. Example of Echoes With Very Low Spectral Width: The 4 October 2002 Event

[16] We have found several good events for the occurrence of ionospheric echoes with very low spectral width during high geomagnetic activity. Among them we will discuss the event on 4 October 2000 in this section. This is mainly because we have echoes over a wide spatial extent at both Syowa East and South during the event period. This is not very common because Syowa South radar has a lower sensitivity than the Syowa East radar. During the period of interest, the radars were operated with the common program, in which each radar scanned through 16 viewing directions every 2 min. Unfortunately, there were very little echoes at CUTLASS radars during this period.

[17] Figure 6a shows the IMF and solar wind parameters observed by the ACE satellite. The ACE satellite recorded a southward turning of IMF at 0400 UT. The IMF stayed constantly southward for the whole rest of the day. The estimated time delay between the ACE satellite and the subsolar magnetopause is 57 min. The geomagnetic activity level (shown in Figure 6b) was quite high on that day. The Kp was 2 to 3+ for the first 6 hours, and 5 to 7+ for the rest of the day. The Dst index showed a gradual decrease from the beginning of the day. It showed a minimum value of −143 nT at 2100−2200 UT, although after a slight recovery it decreased again until the next day. The AL index was constantly high (stayed around 500 nT) from 0400 UT throughout the rest of the day.

[18] Figure 7 shows the RTI plot of the power, Doppler velocity and spectral width of Beam 7 and Beam 8 of the Syowa East and Syowa South radars respectively. The color scale of the spectral width is expanded so that the echoes with low spectral width are easily recognizable. It is seen that there were echoes with very low spectral widths (as low

Figure 1. Distribution of the fields of view of the Iceland East, Finland, Syowa East and Syowa South SuperDARN radars. The magnetic latitude and longitude are given in the Altitude Adjusted Corrected Geomagnetic Coordinate (AACGM) system, which is an updated version of the PACE geomagnetic coordinate system [*Baker and Wing*, 1989]. Also shown are the fields of view of the beams 3 and 5 of the Iceland East, the beam 5 of the Finland, the beam 7 of the Syowa East, and the beam 8 of the Syowa South radars. The data of the hatched area in Iceland East beam 3 and Syowa East beam 7 will be used in the statistical analysis of section 3.1. These two beams are approximately conjugate to each other, although this conjugacy is affected by external conditions and dipole tilt angle.

SYOWA EAST BEAM: 7

DATE : 980101 - 20011231   RANGE : 1000 - 2000 km   TIME : 0:00 - 24:00 UT

Dst-index : all   TOTAL DATA POINTS : 1928269
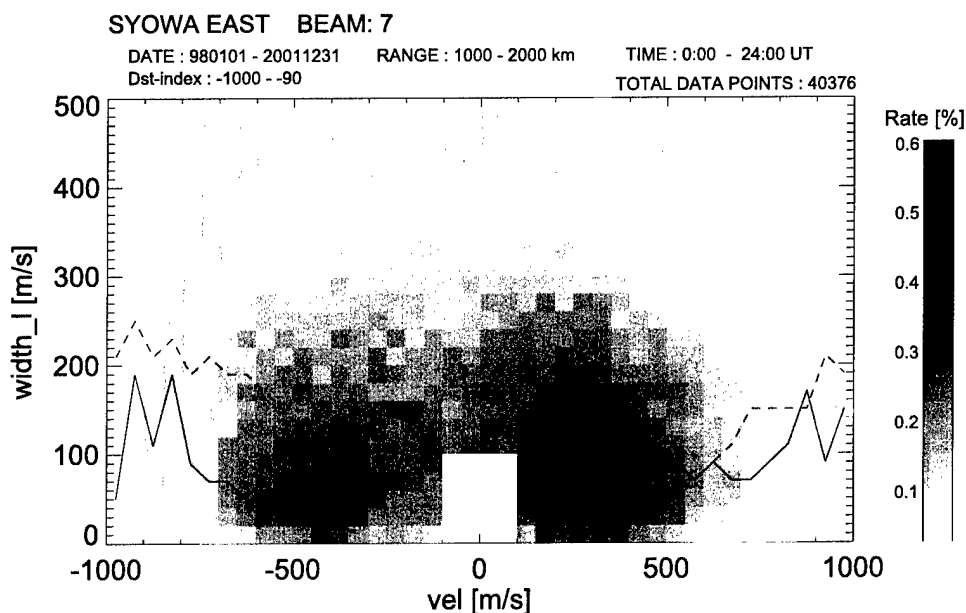
Figure 2. Statistical distribution of the line-of-sight velocity versus the Doppler spectral width obtained with beam 7 of the Syowa East SuperDARN radar. The solid line indicates the peak values of Doppler spectral widths for each velocity range.

as 10 to 20 m/s) between about 1200 UT and 2140 UT. This period corresponds to noon to premidnight sectors.
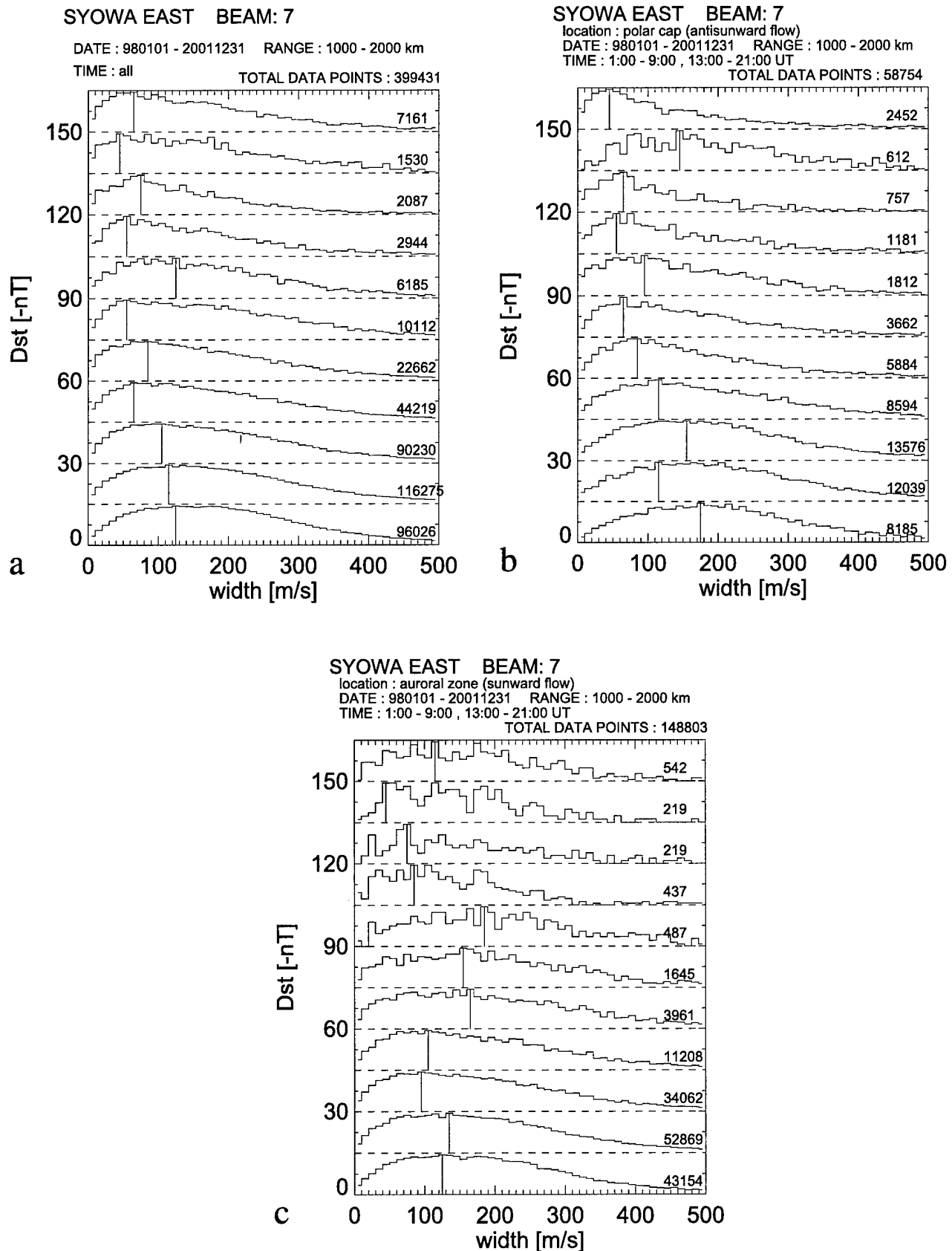
[19] Figure 8 shows the two-dimensional distribution of the line-of-sight velocities (upper panel) and the Doppler spectral width (lower panel) for a 2-min scan during the very low spectral width period. The low spectral width can be interpreted in terms of the absence of turbulent electric field because this effect appeared not only in the low spectral width (lower panel) but also in the Doppler velocity distribution, which shows highly uniform flow which varies sinusoidally as a function of the beam angle. If we assume a uniform flow distribution, the flow direction is expected to

be from north-west to south-east, consistent with the anti-sunward flow in the polar cap region. (Note that the period of interest is during very high geomagnetic activity with Dst = −139 nT).

[20] Figure 9 shows the two-dimensional distribution of the line-of-sight velocities and the Doppler spectral width for a 2-min scan during relatively higher spectral width period. The Dst value was −118 nT, slightly smaller than the period of Figure 8 but still large. The distribution of Doppler velocity is similar to the one shown in Figure 8, but the spectral width is much wider. The velocity distribution along beam 2 for the scan periods in Figures 8 and 9, as

SYOWA EAST BEAM: 7

DATE : 980101 - 20011231   RANGE : 1000 - 2000 km   TIME : 0:00 - 24:00 UT

Dst-index : -1000 - -90   TOTAL DATA POINTS : 40376

Figure 3. Same as Figure 2, but for Dst < −90 nT periods only.

Figure 4. Distribution of the spectral width of ionospheric backscatter echoes for |vel| >= 450 m/s, binned for Dst ranges every 15 nT, obtained by beam 7 of the Syowa East radar. The plots are shown for all the data (a), polar cap data corresponding to the antisunward flow (b), and auroral zone corresponding to the sunward flow (c). The peak value of each distribution is indicated by a vertical line.
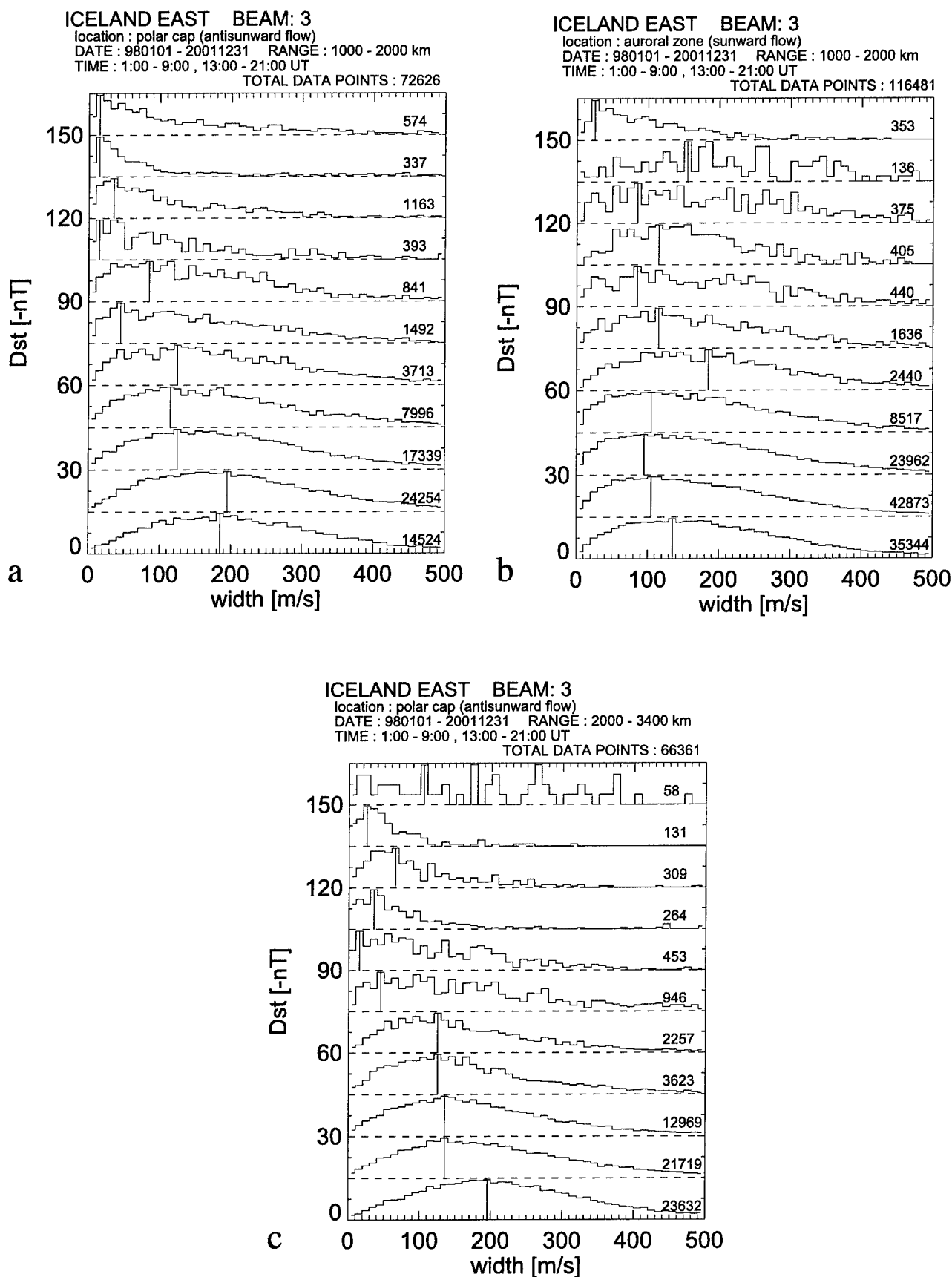
Figure 5. The same as Figure 4, for beam 3 of the Iceland East radar, for the polar cap region (a) and auroral zone (b). Figure 5c is the distribution for the 2000–3400 km range for the polar cap region.
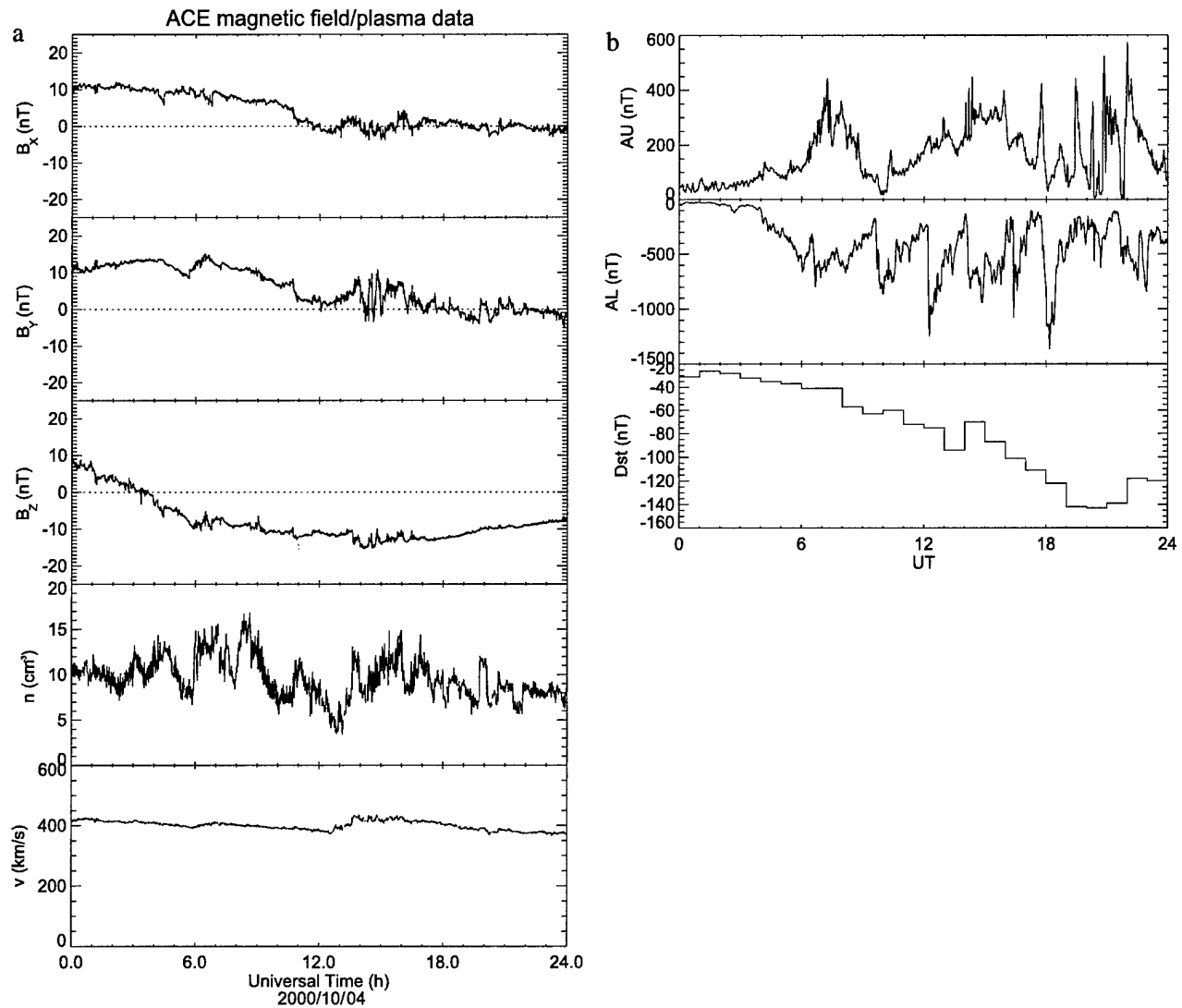
Figure 6. (a) IMF and solar wind parameters observed by the ACE satellite on 4 October 2000. (b) AU/AL and Dst indices on 4 October 2000. The estimated time delay between the ACE satellite and the subsolar magnetopause is 57 min.

illustrated in Figure 10, also shows obvious difference in the characteristics of electric field turbulence between these periods.

[21] We checked the electric field variations observed by the ion driftmeter on board the DMSP-F13 satellite simultaneous with the SuperDARN observation. Figure 11a shows the distribution of the spectral width observed by the Syowa SuperDARN radar (together with the trajectory of the satellite), and Figure 11b shows the horizontal component of the ion drift velocity normal to the satellite path observed by the DMSP-F13 satellite (upper panel) and 6-s standard deviation values (lower panel). We calculated the 6-s standard deviation because when the satellite moves with the speed of 7 km/s, 6 s corresponds to 42 km, which is approximately comparable to one range cell size of the SuperDARN radar (45 km). The DMSP data shows the turbulence level of 0 to 50 m/s in the field of view of the radars (2121–2126 UT) whereas the Syowa SuperDARN data shows the spectral width of about 0 to 100 m/s. It should be noted that the spectral width of the SuperDARN

radar is the result of integration over time and two-dimensional space and does not necessarily coincide with the standard deviation values obtained from the DMSP data.

[22] Figure 12 shows the result of DMSP-SuperDARN comparison during the different period. During this period both data show higher values with the DMSP turbulence level of 50 to 100 m/s and the spectral width of the SuperDARN radars of 50 to 200 m/s. The data period was shortly after the big substorm onset observed by the nightside magnetometer, and the details will be discussed later.

[23] Figure 13 shows the geomagnetic field variation at IMAGE magnetometer network, whose geomagnetic longitude is in the field of view of the Syowa East radar. The data show continuous geomagnetic activity after about 1200 UT, which corresponds to a substorm expansion onset at 1210 UT recorded by GIMA magnetometers in Alaska, progressing poleward to reach the northernmost station at about 1220 UT (data not shown). This approximately coincides with the initial decrease in the

SYOWA EAST RANGE-TIME-PARAMETER PLOT: BEAM: 7
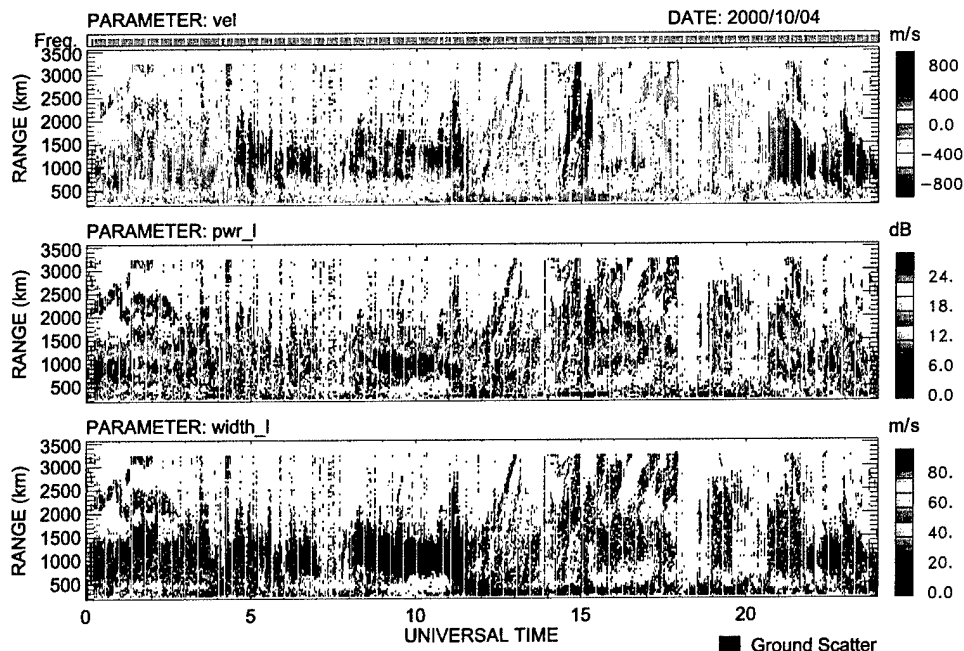
SYOWA SOUTH RANGE-TIME-PARAMETER PLOT: BEAM: 8
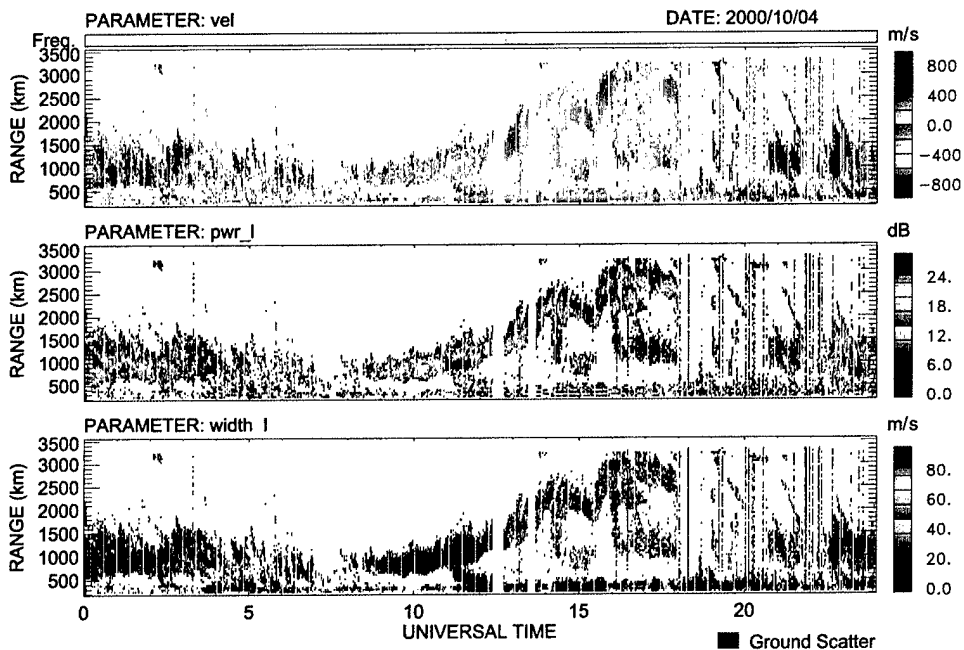
Figure 7. Range-Time-Intensity (RTI) plots of the Doppler velocity, power and spectral width of beam 7 and beam 8 of the Syowa East and South radars on 4 October 2000. See color version of this figure at back of this issue.

spectral width observed by the Syowa East radar at 1218 UT. The starting time of the large disturbance at 14 UT corresponds to an expansion onset observed at 210° MM chain (data not shown). Around this time, the Syowa radars first observed decrease in the spectral width at around 1410 UT and then increase at about 1440 UT. After this, there were several disturbances, some of which can be defined as substorms, but almost all the distur-
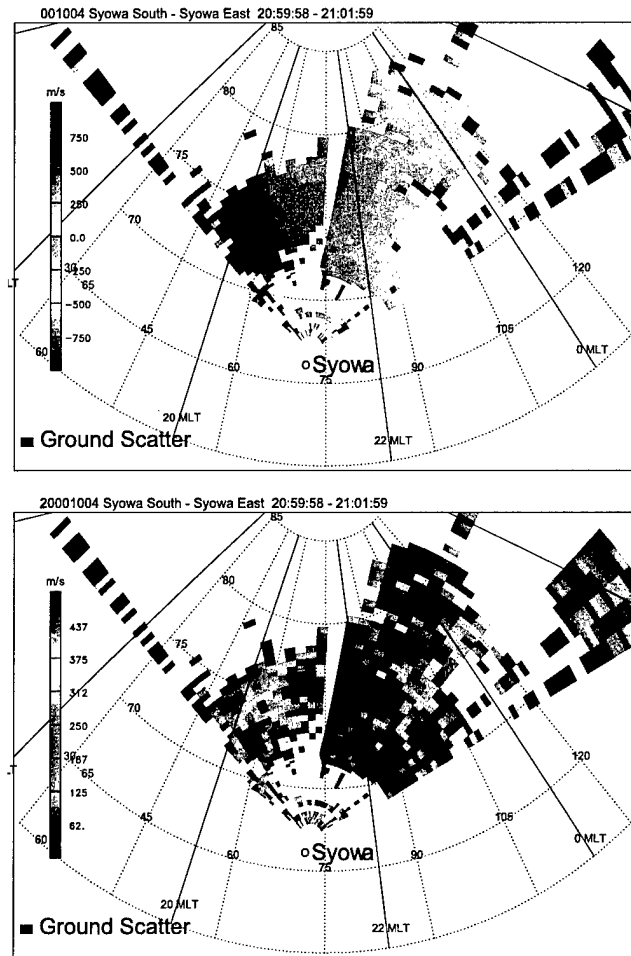
Figure 8. Two-dimensional distribution of Doppler speed (upper panel) and spectral width (lower panel) obtained with the Syowa East and South SuperDARN radars at 2058–2100 UT on 4 October 2000. See color version of this figure at back of this issue.

echoes with high velocity and very low spectral widths were always located in the polar cap region, poleward of the auroral precipitation areas.

3.3. Statistical Result: When Are the Echoes With Very Low Spectral Widths Observed?

[26] In this subsection we show the statistical character-istics of the geomagnetic activity when ionospheric echoes with very low spectral widths were observed. We use the data from the Finland, Iceland East and Syowa East Super-DARN radars for the period of 1 January 1998 to 31 December 2001. We used only the data during the common program period because the shorter integration range might affect the spectral width of each observation cell. In addition, we used only the data for geomagnetic latitude higher than 75° in order to focus on the polar cap data.

[27] We applied the following criteria for choosing the events of ionospheric echoes with very low spectral widths: (1) the amplitude of the Doppler velocity should be larger than 450 m/s, (2) the spectral width should be lower than 60 m/s, and (3) the echoes matching the above two criteria should be observed over at least three consecutive scans and the spatial extent should be more

Figure 9. Two-dimensional distribution of Doppler speed (upper panel) and spectral width (lower panel) obtained with the Syowa East and South SuperDARN radars at 2228–2230 UT on 4 October 2000. See color version of this figure at back of this issue.

bances stayed at relatively lower geomagnetic latitudes (<70°). There was a substorm expansion onset at 2146 UT which reached up to the latitude of 73° (HOR), preceded by the previous onset at 2135 UT recorded by magneto-meters at lower latitudes. Interestingly, this is approxi-mately the timing of the increase in the spectral width in both of Syowa radars. Details will be discussed in the next section.

[24] Polar magnetic field variations are shown in Figure 14. During 2100–2200 UT the satellite was located in the vicinity of geosynchronous orbit. The satellite observed the dipolarization beginning at 2135 UT, corresponding to the initial onset observed by some of the IMAGE magnetometers mainly located at lower latitudes. For the other periods, the satellite was located at much higher latitudes, where it is not easy to detect changes in the magnetic field configuration.
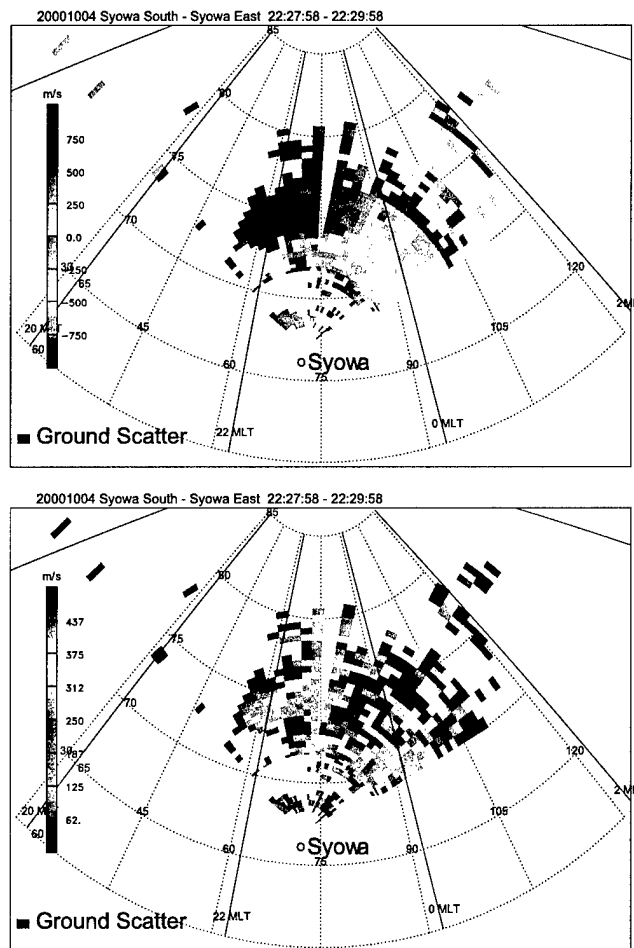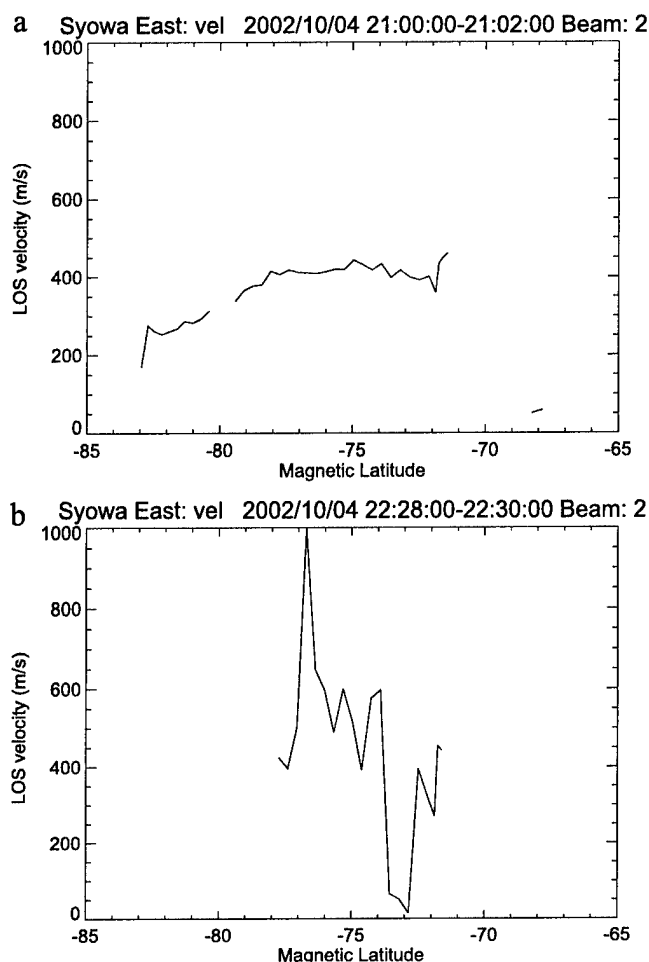
[25] We examined the relative location of the echo region to the particle precipitation pattern. There were a total of 12 passes of DMSP F12, F13, F14, and F15 satellites which crossed the fields of view of the Syowa East and South radars. The DMSP particle data showed that ionospheric

Figure 10. Distribution of the line-of-sight velocities observed at beam 2 of the Syowa East radar (a) during very low spectral width period and (b) during higher spectral width period.

set rather strict criteria for selecting echoes with very low spectral width in order to exclude the effect of ground scatter echoes and E-region echoes. These criteria obviously exclude echoes with high velocity and very low spectral width but with the beam direction almost normal to the background flow vector.

[30] We examined the direction of the flow for the echoes observed in the dusk and dawn sectors by the Iceland East and Syowa radars, whose beams are aligned mainly in the east-west direction. 13 (1) events observed by the Iceland East radar and 17 (3) events observed by the Syowa East radar showed antisunward (sunward) flow. This result also supports that the event of interest occurred preferably in the polar cap region where the antisunward convection prevails.

[31] The typical duration of the events is about 30 minutes to 2 hours, although the 4 October 2000 event was over a period of almost 10 hours. It should be noted, however, that the value of the duration is highly affected by the appearance/disappearance of the echoes and by the

than five range bins. The number of event periods satisfying all the criteria was 24 for Finland, 20 for Iceland East, and 38 for Syowa East radars.
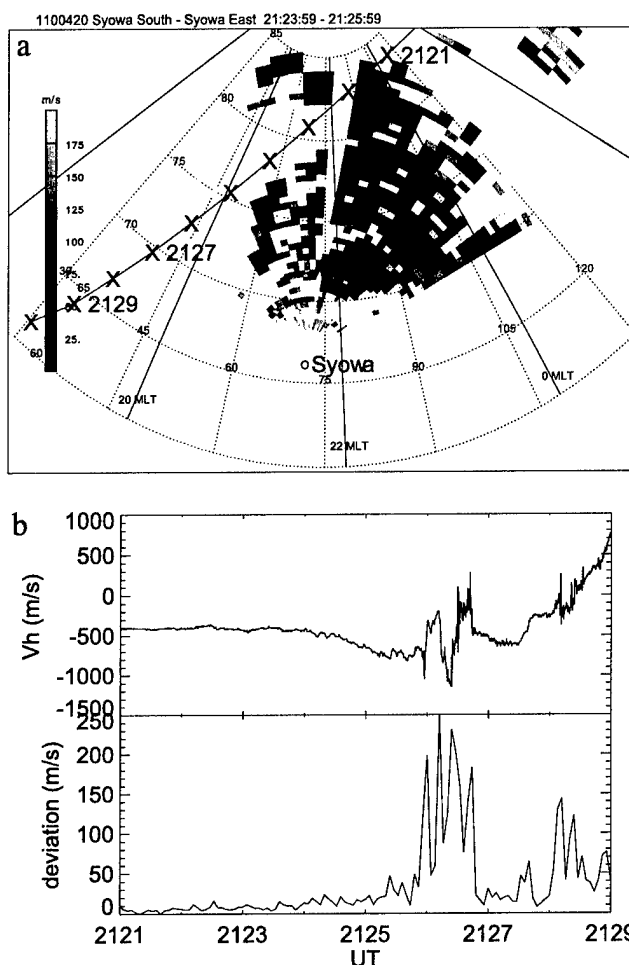
[28] Figure 15a shows the distribution of Dst index during the event periods. This clearly shows that most events occurred during relatively high geomagnetic activity. Figure 15b, plots of the number of events normalized by the occurrence rate of each Dst range, more clearly indicates the close relationship between the occurrence of echoes with very low spectral widths and high geomagnetic activity.

[29] Figure 16 shows the magnetic local time distribution of these events. There seems to be a preferable MLT sector, but it is largely due to a beam angle effect. Finland radar beam 5 is directed meridional, so it is more likely to observed higher velocities in the noon and midnight sectors. The lack of the midnight sector events is probably due to the weak echo power in the nightside region because Finland radar is located at lower geomagnetic latitude than the Iceland East and Syowa radars, so that the echo regions are farther away from the radars. On the other hand, the Iceland East and Syowa East beams are more zonally aligned, so they tend to observe larger velocities in the dawn and dusk sectors. It should be mentioned that we have

Figure 11. (a) Spectral width distribution observed by the Syowa East/South radars for 2124–2126 UT on 4 October 2000. The trajectory of the DMSP-F13 satellite is over-plotted. (b) The horizontal component of the ion drift observed by the DMSP-F13 satellite (upper panel) and its standard deviation for 6 s (lower panel) during 2121–2129 UT.
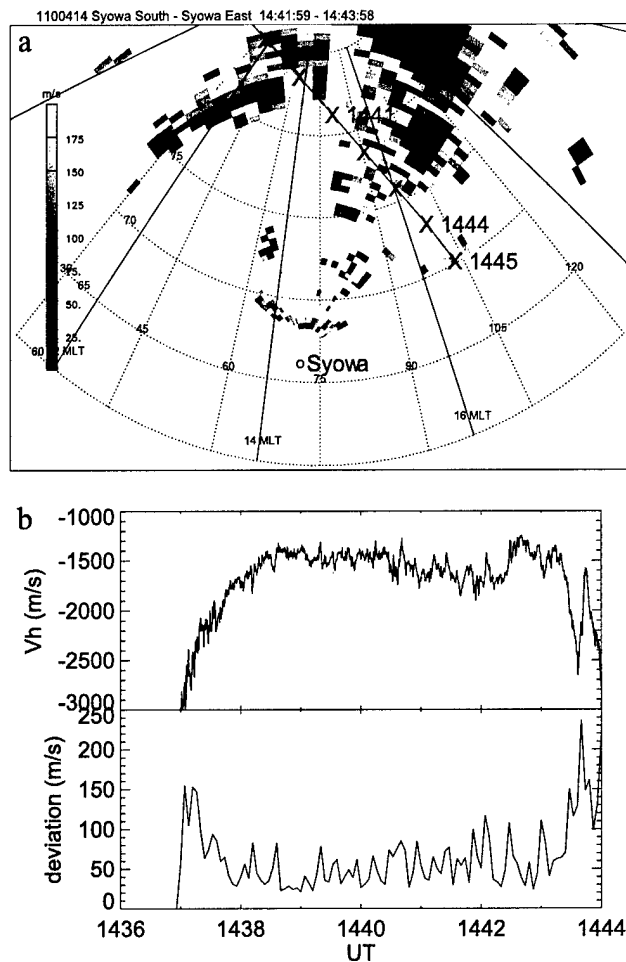
Figure 12. (a) Spectral width distribution observed by the Syowa East/South radars for 1442–1444 UT on 4 October 2000. The trajectory of the DMSP-F13 satellite is over-plotted. (b) The horizontal component of the ion drift observed by the DMSP-F13 satellite (upper panel) and its standard deviation for 6 s (lower panel) during 1436–1444 UT.

beam angle to the flow direction as already discussed in the previous paragraph.

4. Discussion

[32] In this study we reported on the presence of the ionospheric echoes with high velocity and very low Doppler spectral width. The statistical analysis shows that this type of echoes is observed preferentially during geomagnetically active periods. In general it is not easy to observe such echoes because there are several obstacles for identifying such low spectral width echoes. One is the presence of ground scatter echoes together with the ionospheric echoes. The coexistence of the two kinds of echoes will broaden the spectral width. Please note that this type of echoes is not always observed during high geomagnetic activity. One important factor is the disappearance of echoes during active periods possibly owing to the absorption of the HF wave at the D-region ionosphere [*Milan et al.*, 1996]. Such effect can

be seen in Figure 7, for the period of 1800 to 1900 UT and 1940 to 2040 UT.

[33] We used the SuperDARN radar in both hemispheres mainly in order to examine whether there is any interhemispheric difference in the tendency of spectral width during high geomagnetic activity. CUTLASS radars tend to observe lower spectral width values than Syowa radars as reported by *Hosokawa et al.* [2002] and *Woodfield et al.* [2002]. *Hosokawa et al.* [2002] made interhemispheric comparison of the spectral width and concluded that the instrumental effect is less than 30 m/s, but the above effect is not negligible if the spectral width is relatively low (<60 m/s) as in the present analysis. The present study showed that there is no obvious interhemispheric difference in the characteristics of ionospheric echoes with high velocity and very low Doppler spectral width, indicating that the instrumental effect is not significant.

[34] *Davies et al.* [2002] presented a case study of the echoes with low spectral widths in the polar cap region. They highlighted its difference from echoes in the cusp region with high spectral widths although they did not present an explanation for the unusually low spectral widths.

[35] There is a possibility that the echoes with low spectral width observed in this study are E-layer echoes produced by the two-stream instability. These echoes have Doppler velocities around 400 m/s and very low spectral width. The E-layer echoes are usually observed at near ranges, but *Milan et al.* [1997] reported that they are observed also in the far ranges (up to 3000 km), probably owing to the multihop raypaths of the transmitted waves. *Chisham and Pinnock* [2001] also assessed the effects of multihop E-region echoes in the SuperDARN global convection maps, and showed that scatter from the E-region is limited to very near (<1000 km) or farther ranges (>2000 km). However, Figure 8 shows that these echoes are distributed over large spatial extents and are thus unlikely to be of E region origin. Furthermore, we expect the statistical data used in the subsection 3.1, focused mainly on the range 1000–1500 km, to be uncontaminated by E-region scatter.

[36] If these echoes are not E-region ones, then what is the cause of reducing the spectral width? One possibility is the suppression of the small-scale fluctuations by the highly conductive ionosphere. *Weimer et al.* [1985] compared electric field variations at DE-1 and DE-2 satellites conjugate along magnetic field lines, and found that the electric field fluctuations with wavelength of less than 100 km at DE-2 altitude (below 900 km) are more suppressed than those at DE-1 altitude (above 4500 km). They ascribed it to the shielding of the turbulent electric field by the highly conductive ionosphere. However, their argument is mainly in the auroral precipitation region, whereas in the present case the echoes are observed mainly in the polar cap region, and therefore it is unlikely that ionospheric conductivity enhancements are the cause of these low spectral width echoes.

[37] *Golovchanskaya et al.* [2002] made a statistical study of the electric field turbulence in the high latitude ionosphere observed by the DE-2 polar orbiting satellite. They showed that the electric field turbulence level with a spatial scale of 3.8 to 100 km is anticorrelated with
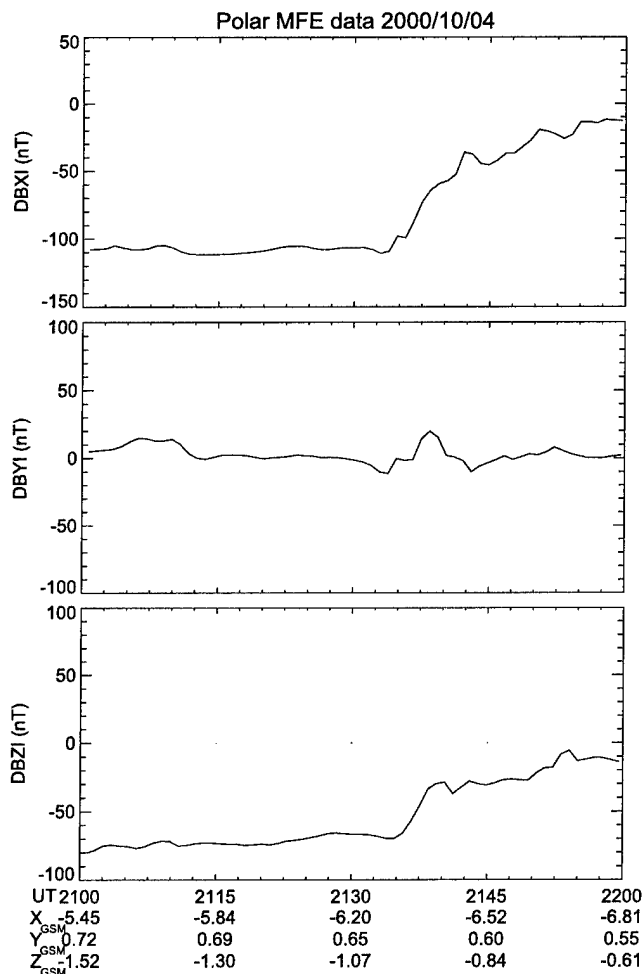
IMAGE magnetometer network 2000-10-04
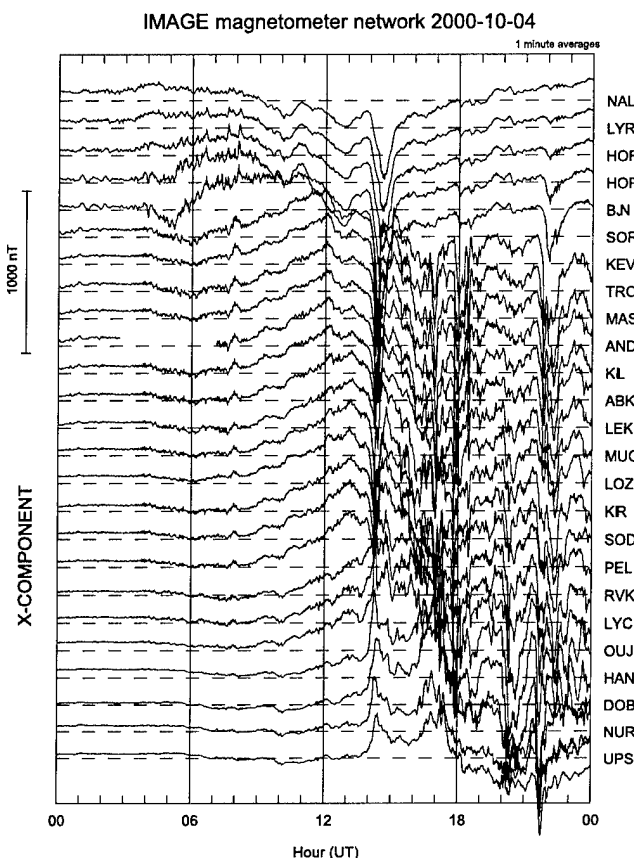
Figure 13. Magnetic field variations recorded at IMAGE magnetometer network on 4 October 2000.

[39] The magnetic field line configuration in the magnetosphere can be examined by using the magnetic field data of the Polar satellite located in the vicinity of geosynchronous orbit. The satellite observed the dipolarization at 2135 UT, corresponding to the preceding substorm onset by magnetometers at lower latitudes. The time delay of the change in the spectral width at 2146 UT relative to the Polar dipolarization can be interpreted in terms of the spatial/temporal effect of the dipolarization region expanding radially and azimuthally with time [*Ohtani et al.*, 1991].

[40] The comparison between the spectral width and the geomagnetic activity for 1200–1400 UT is more complicated because during this period the fields of view of radar were located in the dayside region, far away from the substorm expansion onset region. The dipolarization is first localized in space and then expands radially and azimuthally with time [*Ohtani et al.*, 1991]. The progress of substorms expansion often takes stepwise style rather than gradual/continuous manner [*Wiens and Rostoker*, 1975]. These characteristics of dipolarization might explain why the spectral width decreased corresponding to the expansion onset at 1210 UT and also why this parameter decreased then increased corresponding to the onset at 1400 UT.

geomagnetic activity. They explained their results in terms of the interchange instability which can grow in any curvilinear magnetic field including dipolar and radial plasma density gradient, especially in the presence of the background field-aligned current. They also reported that since the open magnetic field configuration is inconsistent with the instability growth, antisunward flow in the polar cap connected with the open magnetic field lines is laminar. This is consistent with the present results.

[38] *Golovchanskaya et al.* [2002] obtained their results using the polar-orbiting satellite data. With their data set it is not possible to examine temporal variations of the turbulence level in the course of the varying geomagnetic activity. On the other hand, with the radar data it is easy to examine the temporal changes of the electric field turbulence level as a function of geomagnetic activity. Here we examine the dependence of the spectral width on substorm phase, by using the example shown in section 3.2. Figure 13 shows that the timing when the spectral width sharply increased (2140 UT) corresponds to the expansion onset time of a large substorm, in which the disturbance reached up to HOR (geomagnetic latitude ~73°). After the onset of this substorm, the configuration of the magnetic field lines in the polar cap region is expected to change considerably, from tail like to dipolar. If this is so, it is consistent with the theory of *Golovchanskaya et al.* [2002].

**Figure 14.** Magnetic field variation observed by the Polar satellite for 2100–2200 UT on 4 October 2000.
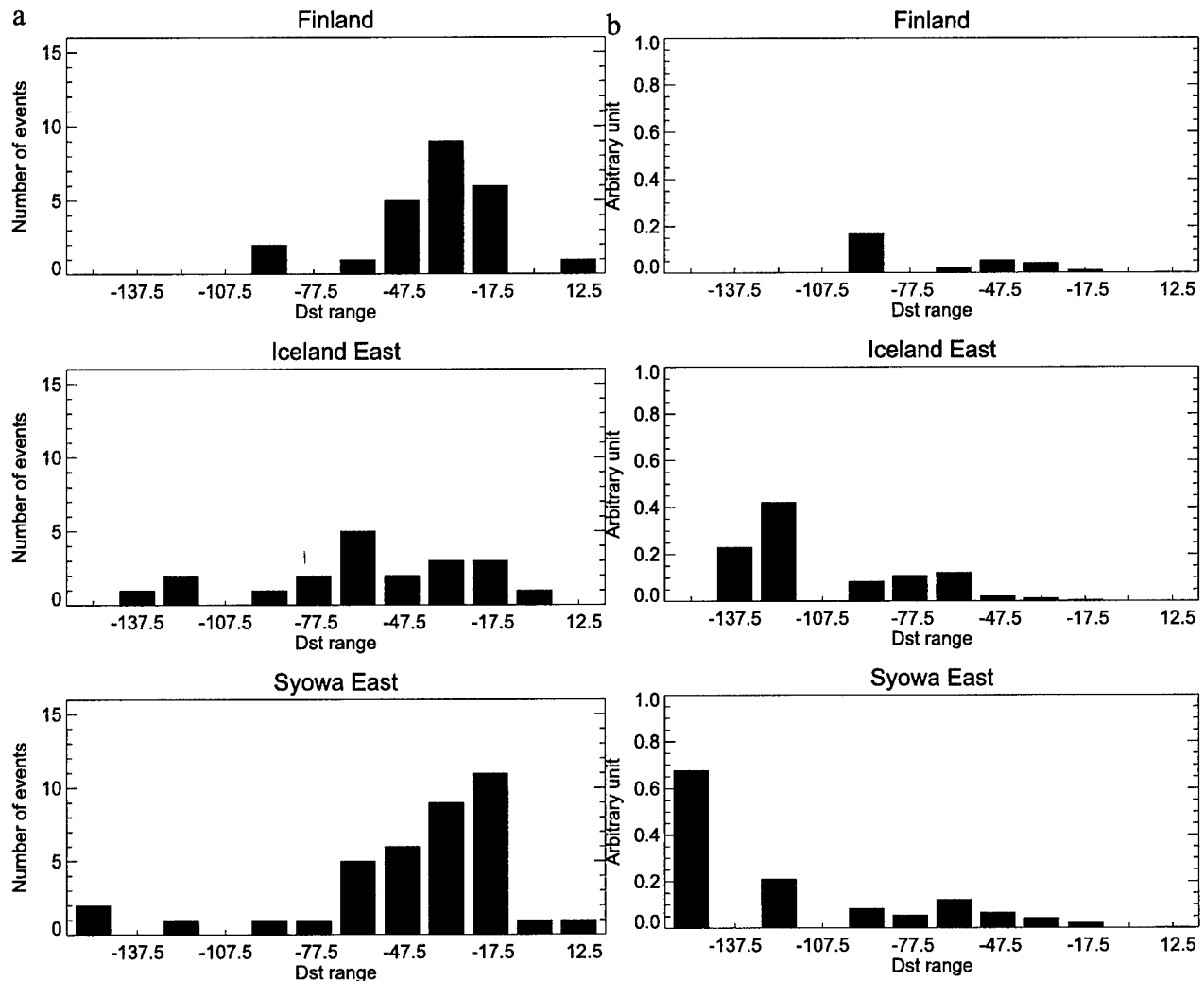
Figure 15. (a) Distribution of Dst ranges for the events of ionospheric echoes with high velocities (>450 m/s) and very low spectral widths (<60 m/s). (b) Same as Figure 12a but normalized by the occurrence rate of each Dst range.

[41] One question arises as to why these echoes with very low spectral width are observed preferably in the polar cap region. There are several factors to increase the spectral width, not only the presence of the electric field turbulence but also the spatial gradient in the electric field [e.g., *André et al.*, 2000]. In the auroral zone, even if the irregular electric field is highly suppressed, the gradient in the background electric field, associated with the field-aligned current, can increase the spectral width. It is not easy to distinguish between the effect of the electric field turbulence and of the electric field gradient on a statistical basis.

[42] Previous statistical analysis [*Woodfield et al.*, 2002; *Hosokawa et al.*, 2002; *Villain et al.*, 2002] have shown that poleward portion of the polar cap (higher than about 80 deg in magnetic latitude) is filled with relatively narrow spectral width irrespective of the level of geomagnetic activities. Actual observations of polar patches on the dayside ionosphere [e.g., *McWilliams et al.*, 2001; *Milan et al.*, 2002] also show this tendency. Consequently, dependence of the spectral width magnitude on the geomagnetic activity seen in the present result could be created by the change in

relative position between radar field-of-view and polar cap region. However, Figure 4 of *McWilliams et al.* [2001] and Figure 2 of *Milan et al.* [2002] show that the spectral width variations inside the polar patches are more likely to be temporal rather than spatial, with the spectral width values changing almost simultaneously over whole patch region. This is also true in the event study of 4 October 2000 in the present paper. Moreover, Figures 11 and 12 shows that the electric field turbulence observed by the DMSP satellite shows obvious difference in the turbulence level although the satellite crossed the high-latitude polar cap region up to −85° geomagnetic latitude. Although the possibility of the spatial effect of the spectral width reported in the previous studies should be considered, their effect is not likely to be significant.

[43] The statistical analysis shows that the occurrence of the echoes with very low spectral width has no outstanding MLT dependence. This is reasonable if the suppression of the electric field turbulence occurs over a global spatial scale, which can be expected when the suppression of the electric field is related to changes in
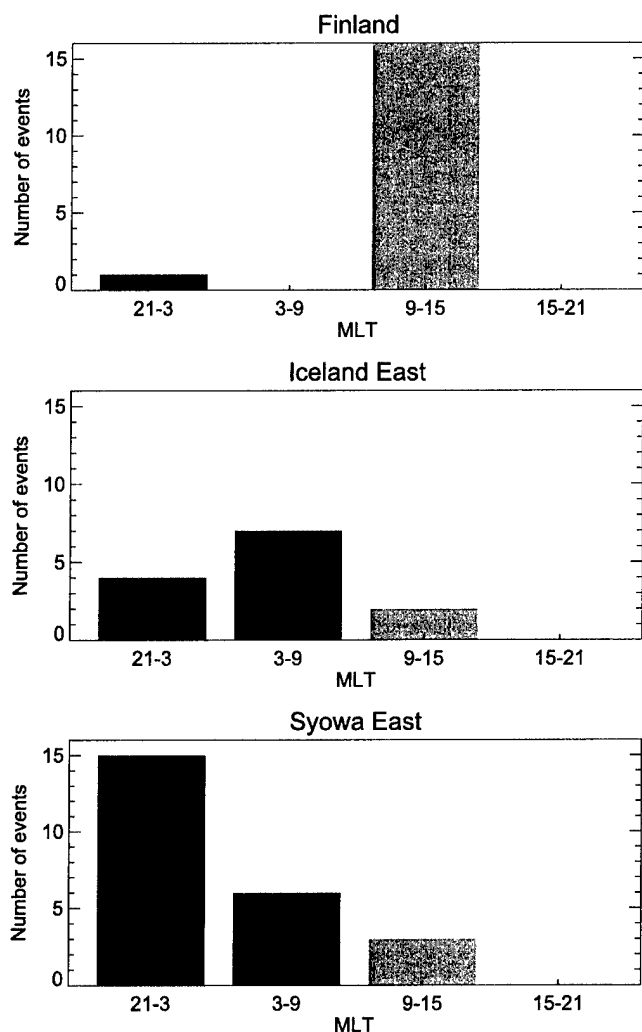
Figure 16. Distribution of MLT for the events of ionospheric echoes with high velocities (>450 m/s) and very low spectral widths (<60 m/s).

the global geometry of the magnetic field lines. Storms can largely affect the geometry of the magnetic field lines in the whole magnetosphere. Substorm effect is mainly on the nightside magnetotail region, but magnetic field lines connected to the polar lobe region also show considerable changes in association with the substorm expansion onset although the delay can be as much as 28 min [*Kawano et al.*, 2002].

5. Conclusion

[44] We have shown the presence of echoes with high velocities and very low spectral widths in the polar cap region during high geomagnetic activity. The event study shows that the appearance of these echoes is closely associated with the suppression of electric field fluctuations. Both the statistical and event study shows that this suppression is highly correlated with the geomagnetic activity.

[45] Although our result is consistent with the previous results by *Golovchanskaya et al.* [2002], further study is necessary to understanding the physical mechanisms of

generating ionospheric echoes with very low spectral widths.

References

André, R., M. Pinnock, J.-P. Villain, and C. Hanuise (2000), On the factor conditioning the Doppler spectral width determined from SuperDARN HF radars, *Int. J. Geom. Aeron.*, 2, 77–86.

Baker, K. B., and S. Wing (1989), A new magnetic coordinate system for conjugate studies at high latitudes, *J. Geophys. Res.*, 94, 9139–9144.

Baker, K. B., J. R. Dudeney, R. A. Greenwald, M. Pinnock, P. T. Newell, A. S. Rodger, N. Mattin, and C.-I. Meng (1995), HF radar signatures of the cusp and low-latitude boundary layer, *J. Geophys. Res.*, 100, 7671–7695.

Chisham, G., and M. Pinnock (2001), Assessing the contamination of SuperDARN global convection maps by non-F-region backscatter, *Ann. Geophys.*, 19, 1–16.

Davies, J. A., T. K. Yeoman, I. J. Rae, S. E. Milan, M. Lester, M. Lockwood, and A. McWilliams (2002), Ground-based observations of the auroral zone and polar cap ionospheric responses to dayside transient reconnection, *Ann. Geophys.*, 20, 781–794.

Fukumoto, M., N. Nishitani, T. Ogawa, N. Sato, H. Yamagishi, and A. S. Yukimatu (1999), Statistical analysis of echo power, Doppler velocity and spectral width obtained with the Syowa South HF radar, *Adv. Polar Upper Atmos. Res.*, 13, 37–47.

Golovchanskaya, I. V., Y. P. Maltsev, and A. A. Ostapenko (2002), High-latitude irregularities of the magnetospheric electric field and their relation to solar wind and geomagnetic conditions, *J. Geophys. Res.*, 107(A1), 1001, doi:10.1029/2001JA900097.

Greenwald, R. A., et al. (1995), DARN/SUPERDARN: A global view of the dynamics of high-latitude convection, *Space Sci. Rev.*, 71, 761–796.

Hanuise, C., J.-P. Villain, J.-C. Cerisier, C. Senior, J. M. Ruohoniemi, R. A. Greenwald, and K. B. Baker (1991), Statistical study of high-latitude E-region Doppler spectra obtained with the SHERPA HF radar, *Ann. Geophys.*, 9, 273–285.

Hosokawa, E. E. Woodfield, M. Lester, S. E. Milan, N. Sato, A. S. Yukimatu, and T. Iyemori (2002), Statistical characteristics of Doppler spectral width as observed by the conjugate SuperDARN radars, *Ann. Geophys.*, 20, 1–11.

Kawano, H., G. Le, C. T. Russell, G. Rostoker, M. J. Brittnacher, and G. K. Parks (2002), Substorm-time magnetic field perturbations in the polar magnetosphere: POLAR observations, *Earth Planets Space*, 54, 963–971.

Lewis, R. V., M. P. Freeman, A. S. Rodger, G. D. Reeves, and D. K. Milling (1997), The electric field response to the growth phase and expansion phase onset of a small isolated substorm, *Ann. Geophys.*, 15, 289–299.

McWilliams, K. A., T. K. Yeoman, and S. W. H. Cowley (2001), Two-dimensional electric field measurements in the ionospheric footprint of a flux transfer event, *Ann. Geophys.*, 18, 1584–1598.

Milan, S. E., T. B. Jones, M. Lester, E. M. Warrington, and G. D. Reeves (1996), Substorm correlated absorption on a 3200 km trans-auroral HF propagation path, *Ann. Geophys.*, 14, 182–190.

Milan, S. E., T. K. Yeoman, M. Lester, E. C. Thomas, and T. B. Jones (1997), Initial backscatter occurrence statistics from the CUTLASS HF radars, *Ann. Geophys.*, 15, 703–718.

Milan, S. E., M. Lester, and T. K. Yeoman (2002), HF radar polar patch formation revisited: summer and winter variations in dayside plasma structuring, *Ann. Geophys.*, *20*, 487–499.

Ohtani, S., K. Takahashi, L. J. Zanetti, T. A. Potemra, R. W. McEntire, and T. Iijima (1991), Tail current disruption in the geosynchronous region, in *Magnetospheric Substorms, Geophys. Monogr. Ser.*, vol. 64, edited by J. R. Kan et al., pp. 131–137, AGU, Washington, D. C.

Villain, J.-P., R. André, M. Pinnock, R. A. Greenwald, and C. Hanuise (2002), A statistical study of the Doppler spectral width of high-latitude ionospheric F-region echoes recorded with SuperDARN coherent HF radars, *Ann. Geophys.*, *20*, 1769–1781.

Weimer, D. R., C. K. Goertz, D. A. Gurnett, N. C. Maynard, and J. L. Burch (1985), Auroral zone electric fields from DE 1 and 2 at magnetic conjunctions, *J. Geophys. Res.*, *90*, 7479–7494.

Wiens, R. G., and G. Rostoker (1975), Characteristics of the development of the westward electrojet during the expansive phase of magnetospheric substorm, *J. Geophys. Res.*, *80*, 2109–2128.

Woodfield, E. E., K. Hosokawa, S. E. Milan, N. Sato, and M. Lester (2002), An inter-hemispheric, statistical study of nightside spectral width distributions from coherent HF scatter radars, *Ann. Geophys.*, *20*, 1921–1934.

Yumoto, K., et al. (2001), Characteristics of Pi 2 magnetic pulsations observed at the CPMN stations: A review of the STEP results, *Earth Planets Space*, *53*, 981–992.

M. Lester and S. E. Milan, Department of Physics and Astronomy, University of Leicester, Leicester LE1 7RH, UK. (mle@ion.le.ac.uk; ets@ion.le.ac.uk)

N. Nishitani and T. Ogawa, Solar-Terrestrial Environment Laboratory, Nagoya University, Toyokawa 442-8507, Japan. (nisitani@stelab.nagoya-u.ac.jp; ogawa@stelab.nagoya-u.ac.jp)

F. J. Rich, Air Force Research Laboratory, Space Vehicles Directorate, 29 Randolph Road, Hanscom Air Force Base, MA 01731-3010, USA. (frederick.rich@hanscom.af.mil)

N. Sato, H. Yamagishi, and A. S. Yukimatu, National Institute of Polar Research, Tokyo 173-8515, Japan. (nsato@nipr.ac.jp; yamagisi@nipr.ac.jp; sessai@nipr.ac.jp)